CHAPTER II
LITERATURE REVIEW

2.1 Flow Accelerated Corrosion (FAC)

Flow-Accelerated Corrosion or Flow-Assisted Corrosion (FAC) was first reported about 40 years ago because there were failures at some plants. An early study was of the flow which induced corrosion in a process for the desalination of seawater.

In the mid-eighties, FAC was more clearly explained by intensive research in the power industry, gas industry, etc. Now, FAC is known as the chemical dissolution of surface oxide and metal, accelerated by flow and flow impingement. It is a mechanism of piping degradation that causes a loss of material from the inside of the pipe and thinning of the wall.

FAC is governed by two major mechanisms: chemical corrosion involving dissolution rate of the oxide layer on the carbon steel pipe wall and mechanical erosion accelerated by fluid flow inside the pipe or high-velocity liquid droplets impinging on the wall. Experimental observations or plant measurements reveal that FAC also depends on the piping layout, local distributions of flow properties, flow chemistry, etc. (Yuh-Ming *et al.,* 1998).

FAC can occur, especially, in high flow rates with turbulent flow and it can be initiated in both single-phase (liquid), and two-phase (steam and water) systems. Liquids or gases that have suspended solid particles will wear or remove the oxide protective film and leave alloy exposed and more susceptible to corrosion. Corrosion rates are usually higher on the outside of pipe bends and tees and at turbulence promoters such as irregular welds or changes in pipe diameter (Shao, 2006).

The FAC in outlet feeders of a power plant can be described as a combination of dissolution-controlled and erosion-controlled corrosion. Dissolution and mass transport may act together and involve convective diffusion, while the erosion component is characterized by the combined action of flow-induced mechanical forces (shear stresses, pressure variation by high flow velocity and particle impact in multiphase flows) and electrochemical processes (Villien *et al.*, 2001).

A scalloped surface supporting a thin oxide layer is observed in many situations involving FAC. Figure 2.1 shows a scalloped surface on the inner surface of a carbon steel feeder pipe.

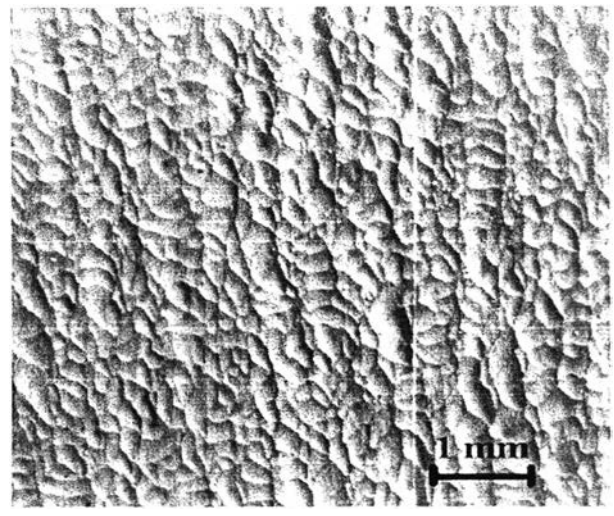

Figure 2.1 Scalloping on the inner surface of a carbon steel feeder pipe (Villien *et al.*, 2001)

2.2 Flow-Accelerated Corrosion (FAC) in outlet feeder pipes of CANDU reactor

The CANDU reactor is a pressurized heavy water reactor, "CANada Deuterium Uranium". This refers to its deuterium-oxide as a heavy water moderator and coolant and its use of uranium as a fuel, originally, natural uranium.

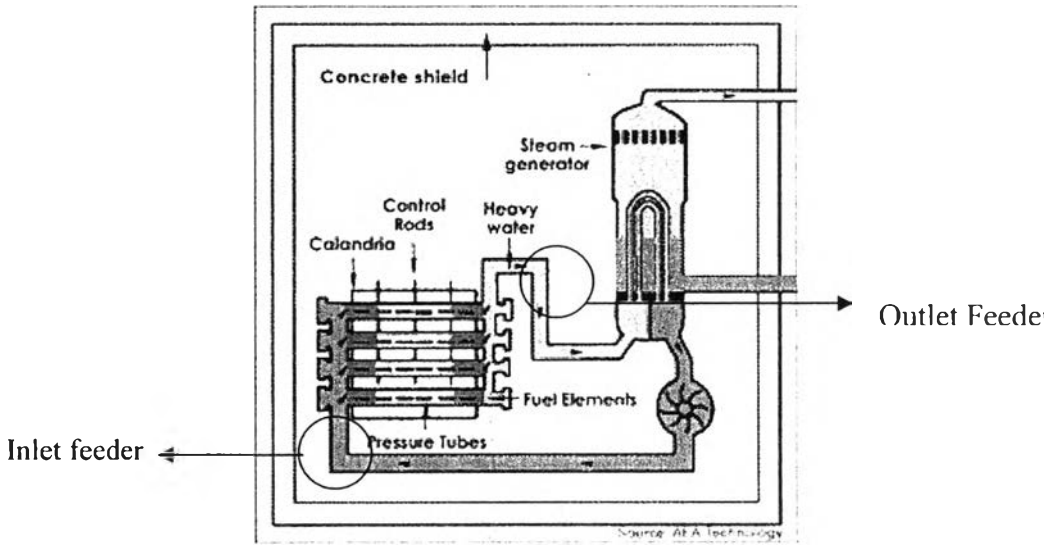

Figure 2.2 Schematic of the primary coolant in a CANDU reactor

Figure 2.2 shows the schematic of CANDU reactor; the heavy water coolant is pumped through the channels containing the fuel elements to pick up the heat generation from the fission reaction and the coolant moves to the steam generators to produce steam from ordinary water and returns to the reactor. The heavy water is expensive but it permits the use of natural uranium as fuel.

In the outlet feeder pipes of CANDU, it has been found that the corrosion is not only uniform but also susceptible to erosion. It has been identified in CANDU primary coolants as the loss of metal from the walls of reactor outlet feeder pipes with high flow velocities.

Measurements on CANDU feeder pipes have indicated that the loss of the metal was often greater than 100 micrometers per year (Lister *et al.*, 1998). This will cause the replacement of the feeder pipes which not only costs more but also involves safety.

During the inspection of the outlet feeders at Point Lepreau during 1996 at positions close to the reactor surface, it was found that excessive thinning of the first few meters of the outlet feeders was widespread due to FAC. Since the discovery, there have been many attempts to understand the mechanism of this FAC and correlate the corrosion rate with operating variables (Lister *et al.*, 1998).

A sample of outlet feeder pipe was kept from the Point Lepreau reactor and analyzed with scanning electron microscope (SEM) images. It shows that the roughness consists of scallops such as are found on secondary side piping that has experienced FAC. Some outlet feeder pipes in Point Lepreau were found to have cracks on the inside surface. Near the cracks, scallops can be clearly seen. Many experiments were subsequently operated to study scallop development and its effect at different parameters such as, pH, pressure, etc.

2.3 Scalloped Surface

Surface scalloping is typical of the attack by FAC of carbon steel. It is also found in the sculpting of clay, mud or rock-river beds by fast flowing streams (Allen, 1971).

Burrill and Cheluget (1998) compared the scallop profiles from feeder pipes and experiments with pipes made from plaster of Paris. They concluded that scallops result from hydrodynamic phenomena and are little influenced by the solid properties.

Villien *et al.* (2001) studied 367 populations of scallops in plaster test sections and the results showed that the scallops were typically 0.56mm long and 0.34mm wide. This suggests that scallop characteristics should be used as a relevant parameter for the description of the scalloping phenomenon rather than the width and they found that the size of defects in the surface of plaster also influenced scallop formation. At a given flow rate, smaller sand particles embedded produced smaller scallops. Moreover, water flow rate affects the size and number of scallops. The number of scallops increased with the flow rate whereas the average size of a scallop decreased with the flow rate. Some defects are erased from the surface after a given time and only scallops bigger than a critical size, set by the flow conditions, remain at the surface.

2.3.1 Geological Studies

The erosion situations have been studied in many disciplines such as geomorphology, geology, aeronautics and civil, mechanical and chemical engineer-

ing. The reason is that the several processes of erosion are physically analogous and often lead to similar surface markings.

There are 2 theories that describe space, size and shape as shown in Figure 2.3.

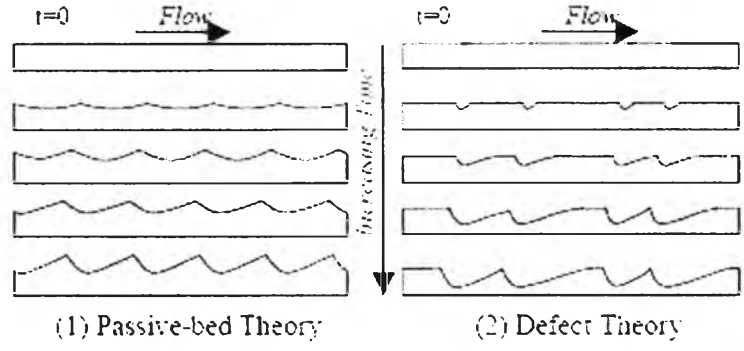

Figure 2.3 Evolution of a surface, (1) passive-bed theory and (2) defect theory

2.3.1.1 The Passive-bed Theory

Scallops on the surface were originally believed to be imprints of the hydrodynamics characteristics of the flowing fluid but Sharp (1947) and Leighly (1948) proposed that the characteristics of scallops on ice surfaces were controlled by the properties of vortices in the adjacent air and Henderson and Perry (1958) support the same idea with studies of meteorites and limestone caves.

Curl (1966) suggested the passive-bed theory of erosion marks, which postulates that the characteristics of the erosion marks are entirely determined by the dynamic properties of the fluid in contact with the surface. There are no influences and effects of the properties of the material on the formation of the scallops. The length of the erosion marks is assumed constant with time.

Allen (1971) found that spatially periodic flow exists, in the attached boundary layer, only within the range of Reynolds number close to laminar-to-turbulent transition. That means the passive theory can be used, for flow imprinted on the surface, only in this condition.

2.3.1.2 The Defect Theory

The defect theory postulates that the position of each erosion mark is due to the initial presence of an irregularity or a defect at the surface. Allen (1971) supported the defect theory and found that the characteristics of any assemblage of scallops depend on three things: the duration of the eroding phenomenon, the spatial distribution of the defects and the flow characteristics.

Villien *et al.* (2001) supported the defect theory that no scalloping can occur if there is no driving force for the dissolution process and, in 2005, they found that scallops are difficult to initiate on the surface of reference plaster due to the absence of initial artificially created defects; that means that hydrodynamics of the fluid alone cannot initiate the scalloping phenomenon but may influence it after the process is started by dissolution.

Shao (2006) studied the origins of scallops and found that scallops originated from surface imperfections (probably air bubbles or impurity material). Allen (1971) proposed a defect model that postulates that there is a population of flaws on the surface. Under certain flow conditions, these flaws will grow and evolve into scallops.

2.3.2 Flute

Scallops can naturally occur with water dissolving limestone or air subliming ice. In either case, surface irregularities may lead to the flow situation in Figure 2.4.

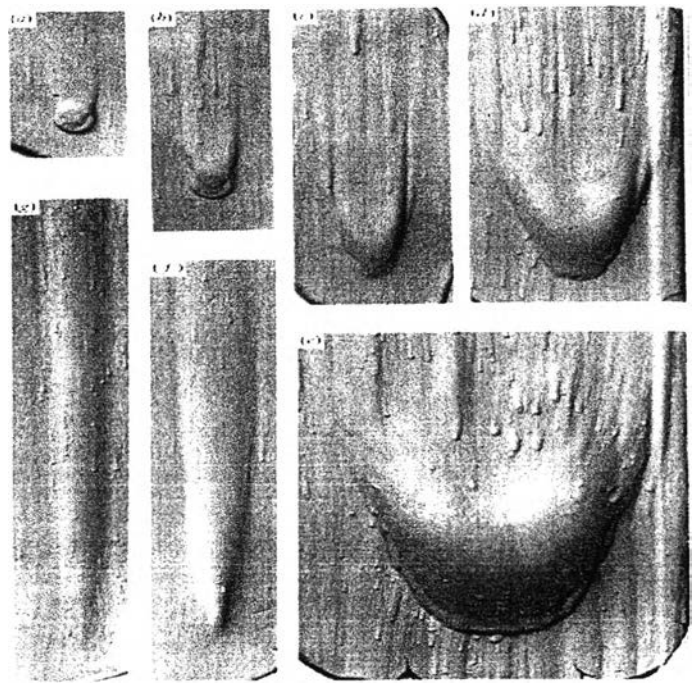

Figure 2.4 Stages in the development of experimental flutes (a-e) and grooves (f), (g) defects introduced into Plaster of Paris beds. Flow from bottom to top. (e) 10cmwidth (Allen, 1971).

A flute is a defect that exceeds a certain critical dimension set by flow conditions and grows by length, breadth and depth into a heel-shaped hollow with a parabolic plan. Allen (1971) found that flutes on the surface resulted from defects changing into scallops.

Curl (1974) explained the characteristic scaling of scallops such that if the velocity is low, transition to turbulence (Point 3 in Figure 2.5) will occur further along the scallop and reattachment will impinge on the next crest. The higher corrosion rate at that point will reduce the crest and, in effect, lengthen the scallop. On the other hand, if the velocity is high, transition and reattachment will occur sooner. In this case, the distance between the reattachment (Point 4) and the next crest will be increased and an irregularity in this region could be the origin of a new scallop, thereby reducing the average scallop size. See Figure 2.5.

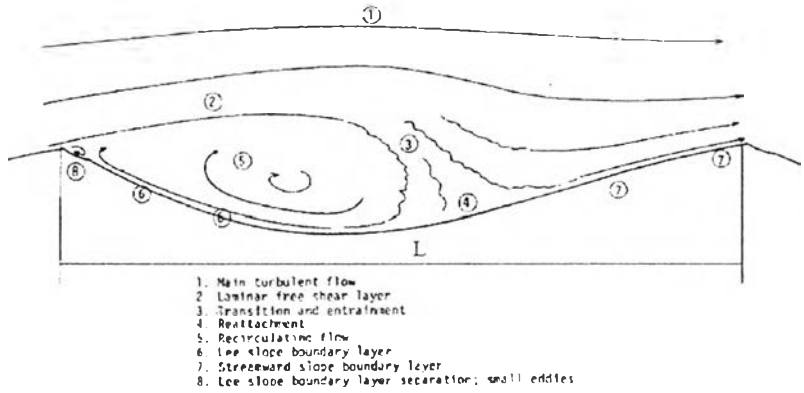

Figure 2.5 Flute hydrodynamics (Blumberg, 1970)

Blumberg (1970) studied the hydrodynamic factors affecting the original propagation of the flute. He tried to obtain a stable fluted surface and found that by using a knife to create a series of grooves perpendicular to the flow direction, a stable dissolution profile flute could be created. Another important conclusion is that there is a stability wavelength Reynolds number for flute stability which is about 23,000 (Blumberg and Curl, 1974). This agrees with that obtained from ice and limestone. They proposed that the number 23,000 could be a universal Reynolds number for an equilibrium erosion surface.

Sato (1956) and Becker and Massaro (1968) studied unstable laminar shear layers and found that the distance between the separation and reattachment points are about 6.5 times the thickness of the boundary layer.

2.4 Plaster of Paris ($CaSO_4.½H_2O$)

Plaster of Paris is calcium sulphate hemihydrate, $CaSO_4.½H_2O$, as a calcined gypsum having a purity of not less than 95% $CaSO_4·½H_2O$ by mass. It consists of calcined gypsum with small amounts of additives (less than 5% by mass) to modify physical characteristics. To produce a plaster, slurry can be formed to the desired shape and will have a hard, rigid structure.

Plaster of Paris was chosen to study many phenomena, such as to predict the effects of hydrodynamics on the dissolution of pipe walls (Coney *et al.*, 1982), be-

cause of its advantages. For example, plaster of Paris is easy to cast to a suitable size and shape, furthermore it is inexpensive and replacement of the test sections can be easily made. Moreover, the solubility of the plaster in water is reasonable and significant and it can be obtained in a short period of time.

Plaster of Paris, which is used for this project, is produced by Fisher Scientific Company as a pure white plaster with less than 5% additives. When plaster is mixed with water, a reaction takes place and water is absorbed by the calcium sulphate hemihydrate to form the dihydrate generally referred to as gypsum.

$$CaSO_4 \cdot {}^1/_2H_2O + {}^3/_2H_2O \longrightarrow CaSO_4 \cdot 2H_2O$$

Plaster of Paris *Gypsum*

The final product is a coherent mass of needle-shaped gypsum crystals as shown in Figure 2.6.

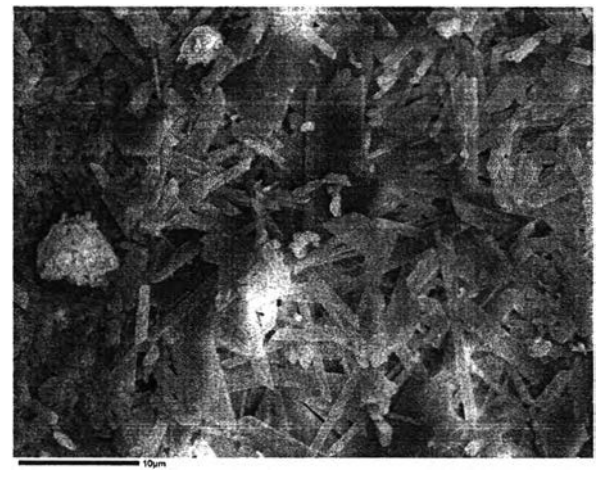

Figure 2.6 SEM micrograph of the plaster structure.

The dissolution of gypsum in pure water is usually represented as;

$$CaSO_4 \cdot 2H_2O \longrightarrow Ca^{2+} + SO_4^{2-} + 2H_2O$$

Calcium ion is analyzed by Atomic Absorption Spectrometry (AAS) to get the concentration and to be converted to rate of dissolution. We neglect reactions associated with the dissolution of carbon dioxide because they affect the interaction between gypsum and water.

2.5 Dissolution of Plaster

The dissolution rate of a solid into an aqueous solution without any more reaction is controlled by the chemical reaction at the surface or by molecular diffusion through the boundary layer. In both cases, rate of the solute transport through the boundary layer, at steady state, will be equal to the mass flow of the dissolved material at the surface.

Two extreme cases exist. When the diffusion transfer is high enough to ensure that the surface concentration of the dissolved species is close to that in the bulk flow, the rate of dissolution is controlled by the reaction rate at the surface. On the other hand, when the diffusion transfer is relatively low and/or the rate of dissolution of the surface is high, molecular diffusion becomes the limiting step. An increase in the fluid velocity will thus enhance mass transfer (Villien *et al.*, 2001 and 2005).

Dissolution of plaster in water has been studied extensively. Early studies showed that the dissolution kinetics is transport-controlled and a first-order rate equation for the dissolution rate is often proposed (Liu and Nancollas, 1971; Christoffersen and Christoffersen, 1974; James and Lupton, 1987; Opdyke *et al.*, 1987);

$$R = k_t(C_s - C_b) = \frac{D}{\varepsilon}(C_s - C_b) \tag{1}$$

where R is the overall dissolution rate, C_s is the concentration at the surface, C_b is the concentration of dissolved species in the bulk, k_t is the mass transfer coefficient, ε is the diffusion layer thickness and D is the diffusion coefficient through the boundary layer. This has been supported by the observed dependence of the overall dissolution rate on the thickness of the diffusion layer. A thinning of the layer at the dissolving surface results in higher dissolution rates. An increase of the fluid velocity will de-

crease the thickness of the boundary layer, and the concentration gradient in the boundary layer becomes steeper.

Recently, Raines and Dewers, (1997) and Jeschke *et al.* (2001) argued that the dissolution of gypsum is jointly controlled by the surface reaction and the diffusion transport through the diffusion layer. The effective gypsum dissolution rate is then determined by "mixed" kinetics. Assuming a second-order reaction, the dissolution rate of gypsum is expressed by (Raines and Dewers, 1997):

$$R = k_t\left(1-\Omega^{1/2}+\zeta\left[1-\left\{1+\frac{2.\left(1-\Omega^{1/2}\right)}{\zeta}\right\}^{1/2}\right]\right) \tag{2}$$

where k_t is the transport coefficient for purely transport control, ζ is the transport reaction factor and $\Omega = C_b/C_s$. The factor ζ measures the relative influence of transport and reaction processes and is expressed as:

$$\zeta = \frac{Dm_{eq}}{2\varepsilon k_t} \tag{3}$$

where m_{eq} is the molal equilibrium concentration.

Raines and Dewers (1997) suggested that there is a 5-step process to chemically interact minerals with moving fluids. First, reactants in the fluid must cross a hydrodynamic boundary layer to reach the mineral surface. Second, reactants must be adsorbed onto the mineral surface. Next, a chemical reaction must take place. Then, the products are formed and released from the surface. Finally, the products must be transferred across the hydrodynamic boundary layer and into the bulk solution. For the case of the gypsum-water system, the reactants are H_2O and $CaSO_4{\cdot}2H_2O$. The products are Ca^{2+} and SO_4^{2-} ions.

Villien *et al.* (2005) studied the dissolution rates of plaster with four different liquid flow rates in a closed re-circulating system and found that the dissolution rates of gypsum decreased approximately exponentially as the concentration of Ca^{2+} increased. As shown in Figure 2.8. the gypsum dissolution is under mixed trans-

port/reaction control, where the transport-controlled kinetics dominates the initial dissolution, and surface reaction kinetics become more important as the concentration of Ca^{2+} increases, which is in agreement with Raines and Dewers (1997).

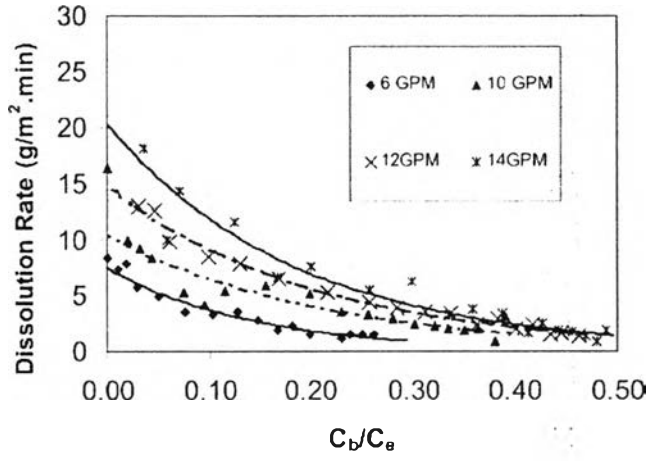

Figure 2.7 Dissolution rates of gypsum as functions of flow rate (Villien *et al.*, 2005).

In addition, with the assumptions of first-order and second-order reactions at the surface of gypsum, expressions (1) and (2) respectively, their results showed that equation (2) or a second-order reaction was found to describe better the kinetics of dissolution for plaster of Paris, but seems to overestimate the dissolution rate as the solution approaches saturation.

Raines and Dewers (1997) found that the rates of dissolution of two alabaster gypsum samples are similar, while the "porous" gypsum and anhydrite samples display lower steady-state concentrations and consequently lower dissolution rates, as shown in Figure 2.8. From their results, it can be seen that the experiments achieved a steady state after about 4 hours. Different physical characteristics of gypsum, caused by different amounts of impurity and porosity, in general cause it to dissolve at a faster rate than anhydrite.

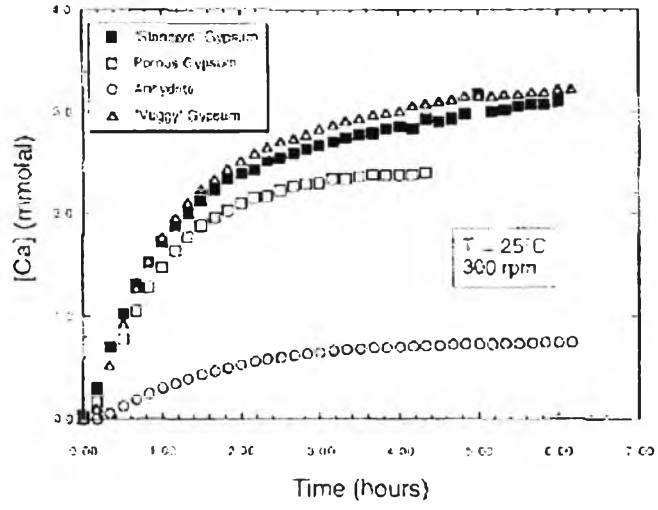

Figure 2.8 Concentration of calcium ion vs time for four experiments, each run at 300-rpm spinning rate and 25°C (Raines and Dewers, 1997)

Shao (2006) found that scallops developed very fast at the beginning of a test (plaster of Paris, within 1 hour), which corresponded to a quick increase of water conductivity. He suggested that a higher driving force for mass transfer occurred in the beginning of the test, which was reduced when the dissolution of plaster of Paris increased the Ca^{2+} and SO_4^{2-} ion concentrations. In addition, he found that the inlet and outlet for fluid flow in the pipe had different scalloping types, which suggested that the scalloping profile is related to the dissolution rate and the higher turbulence within the entrance length may induce higher dissolution.

Figure 2.9 Schematic of different scallop types at inlet and outlet (Shao, 2006).

Azimi *et al.*, (2007) compared the solubility of calcium sulphate as determined using OLI software and mixed solvent electrolyte (MSE) model. Gypsum solubility was as shown Figure 2.10.

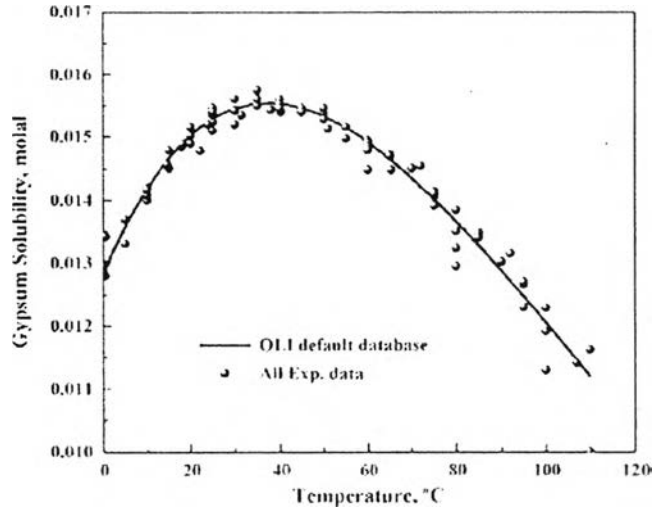

Figure 2.10 Dihydrate solubility in H_2O vs. temperature. The curve is determined-from the OLI default database (Azimi *et al.*, 2007)

Sinthuphan (2008) found that the dissolution rates increase with time because of the increasing plaster surface. Moreover, the different flow rates present different dissolution rates. It indicates that the diffusion transport is the limiting step because the dissolution rates increase with the flow rates.

2.6 The Effect of Temperature

Lebedev and Lekhov (1989) studied the dissolution kinetics of natural gypsum in water at 5-25 °C and found that the temperature dependence of the rate constant fits an Arrhenius equation. The activation energy of 10-11 kcal/mol appears to correspond to mixed dissolution kinetics. Moreover, the rate constant seems to be proportional to the temperature, as in Liu and Nancollas's (1971) work where the rate constants were analysed with the Arrhenius equation at temperatures between 10° and 30°C. The activation energy was found to be Ea = 10±1.5 kcal/mole, which is larger than the value of 4.5 kcal/mole, to be expected on the basis of pure mass transport control for which only the temperature dependence of the diffusion coefficient should be important as shown in Figure 2.11. Although much of the evidence points to diffusion across the liquid boundary layer as being the rate controlling step

in the dissolution of calcium sulphate dihydrate, it is not possible in the light of this relatively large activation energy. It is a more complicated mechanism.

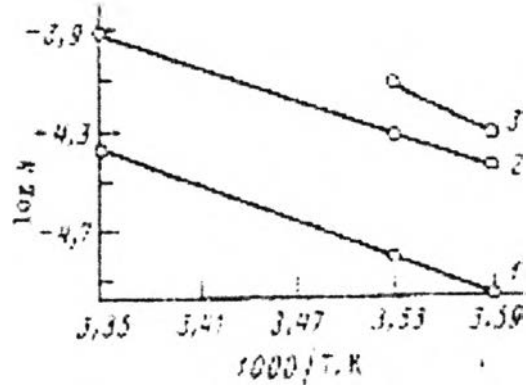

Figure 2.11 The 1000/T dependence of log k (dissolution rate constant) of different specimens or different kinds of gypsum (Lebedev, *et al.* 1989).

2.7 Pressure Drop

Shao (2006) studied the effect of scalloping on pressure drop. The author found that the pressure drop increased at the beginning and became stable for Run 1 but decreased in Run 2, as shown in Figure 2.12.

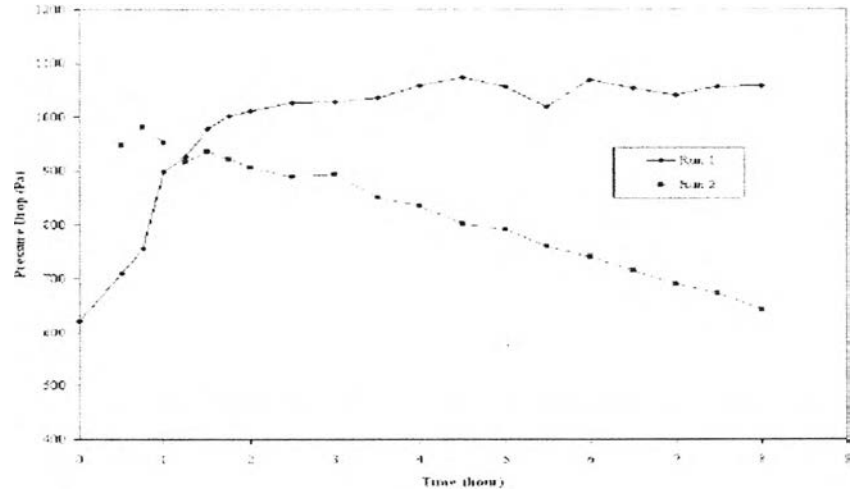

Figure 2.12 The pressure drop versus time (Shao, 2006)

These two runs operated at the same conditions but had different types of plaster of Paris; Run 1 was a pure plaster of Paris (98% $CaSO_4 \cdot \frac{1}{2}H_2O$) and Run 2 was a commercial plaster of Paris containing impurities such as sand. It seems that Run 2 gave high scalloping but less resistance. It appears that hydrodynamic forces could make the plaster surface less resistant. However, the difference between Run 1 and Run 2 was not fully explained.

Shao (2006) proposed that if the scalloping can make the surface smoother, a scalloped surface could be the best candidate to give the highest ratio of k/f (mass transfer coefficient to friction factor) for a given roughness height. This ratio can make the scalloped surface a desired choice for high mass transfer with a low pressure drop.

Lertsurasakda (2007) investigated the effect of scallop distribution on pressure drop using machined tubular sections and found that the pressure drop mainly depends on the surface geometry, not the position. The pressure drop of a scalloped surface depends on the scallop surface area and is almost unaffected by the scallop distribution. He also studied the effect of scallop surface area with forward and backward flow on the pressure drop. He found that the friction factors obtained from backward and forward flow are not the same, even though they have the same roughness height. The friction factors calculated from the experiment are not equal to those calculated from the Von Karman equation for fully rough surfaces in turbulent flow, which give a constant value of the friction factor at high Reynolds numbers.

2.8 The Effect of pH

Azimi *et al.*, (2007) found that the solubility of $CaSO_4$ hydrate in H_2SO_4 solution at low temperature (25-60°C) increased moderately with the addition of H_2SO_4. However, the solubility was decreased at high concentration of acid. The solubility is shown as Figure 2.13.

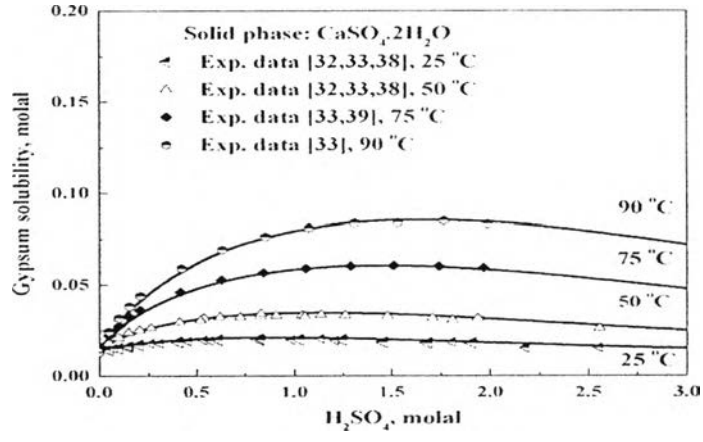

Figure 2.13 Gypsum solubility in H_2SO_4 solutions at different temperatures (Azimi, 2007).

Rechenberg and Sprung (1983) found how the solubility of calcium sulphate depends on alkali hydroxide concentration. The solubility of calcium decreased as the alkali hydroxide concentration increased as shown in Figure 2.14.

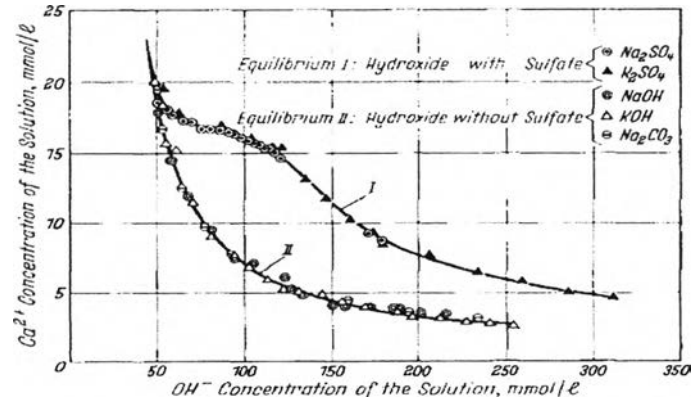

Figure 2.14 Dependence of Ca^{2+} concentration on the OH^- concentration in the solution with and without sulphate (Rachenberg and Sprung, 1983).

Sinthuphan (2008) found that the population of scallops is reduced by an increasing pH. The dissolution rate increases with time in acid and neutral solutions but decreases initially before stabilizing in a basic solution. The average dissolution rate decreases with decreasing temperature and is samewhat affected by pH as shown in Figure 2.15.

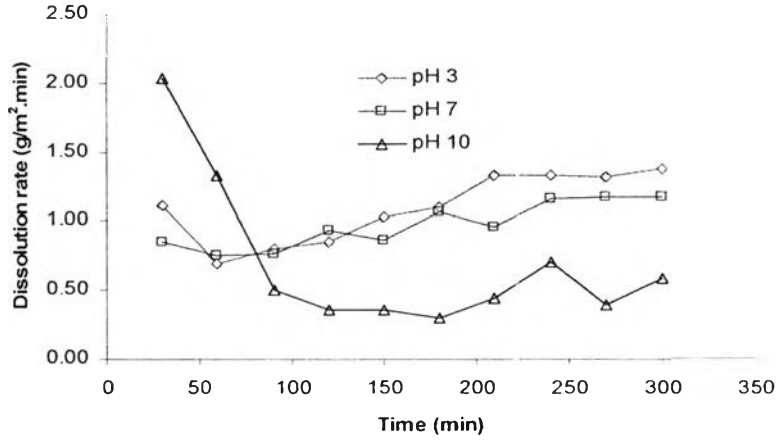

Figure 2.15 Comparison of dissolution rates at different pHs (Sinthuphan, 2008).